Electronic Supplementary Material (ESI) for New Journal of Chemistry.

Supplementary Materials

Multifunctional applications of amino functionalized $Ti_3C_2T_x$: high flux oil/water separation and dye removal

Zhen-Hui Liu[1], Wei-Qiu Cai[1], Qing-Ming Wang, Qiu-Feng Lü*

College of Materials Science and Engineering, Fuzhou University, 2 Wulongjiang North Avenue, Fuzhou 350108, China

[1] Zhen-Hui Liu and Wei-Qiu Cai contributed equally to this work.

* Corresponding author.

E-mail address: qiufenglv@163.com, qiufenglv@fzu.edu.cn.

Text

2.1. Materials

Ti_3AlC_2 (500 meshes) was purchased from Laizhou Kaiene Ceramic Materials Co., Ltd. Hydrofluoric acid (HF, AR, ≥40%) was provided by Aladdin Industries. *N*-[3-(Trimethoxysilyl)propyl]ethylenediamine (AEAPTMS), kerosene, and ketroleum ether were purchased from Shanghai Aladdin Biochemical Technology Co., Ltd. Malachite green (MG), acid blue 74 (AB), methylene blue (MB), congo red (CR), orange-yellow G6 (AO), Sudan III, NaCl, HCl, $NH_3 \cdot H_2O$, NaOH, absolute ethanol, *N*-hexane, cyclohexane, pump oil, *N*-heptane, dichloromethane and trichloromethane were obtained from Sinopharm Chemical Reagent Co., Ltd. PU sponge was obtained from Hebei Yuda Polyurethane Products Co., Ltd., China, and it was divided into small cubes of 12 mm^3 or 32 mm^3, and washed using deionized water (DIW) and absolute ethanol, respectively, before use. Mixed cellulose ester (MCE, a mean pore size of 0.22 μm) membranes were purchased directly from Shanghai Xinya Purification Devices Co., Ltd., China, and washed using deionized water and absolute ethanol before use.

2.6. Characterization

The morphologies of powders, sponges and membranes were observed by using field emission scanning electron microscopy (FE-SEM, Carl Zeiss ULTRA 55). The crystal structures of the samples were characterized by X-ray powder diffraction (XRD, Ultima III) at a test voltage of 40 kV, and a scan rate of 5° min^{-1} in the 2θ range from 5° to 80°. The samples were characterized by Fourier Transform infrared spectroscopy (FT-IR, Nicolet 5700, Nicolet, USA) to detect functional group information in the samples. X-ray photoelectron spectroscopy (XPS, K-Alpha+, Thermo Fisher Scientific) employed a monochromatic AlKa (1486.71 eV) source to record sample photoelectron spectra under high vacuum conditions. Thermogravimetric analysis (TGA) was

performed on a Netzsch STA449C thermogravimetric analyzer at a heating rate of 10 °C/min from 30 °C to 800 °C under nitrogen atmosphere. Thickness measurements were done using an electronic digital micrometer. A Malvern particle sizer (NanoZS 90, Malvern Instruments, British) was used to study the charge carried on the surface of the material at different pH values. A contact angle goniometer (SL200B, Kono Industries, USA) was used to measure the water contact angle (WCA) in air, oil contact angle (OCA) in water and under water oil contact angles (UWOCA) of the sample. The concentration of dyes in the raw material solution and filtrate was characterized by UV-Vis spectrometer (Lambda 950，PerkinElmer).

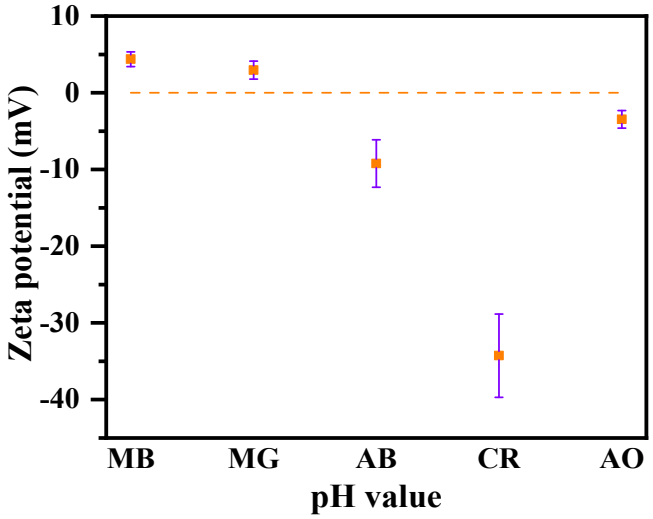

Fig. S1. Surface charges of MB, MG, AB, CR, and AO aqueous solutions.

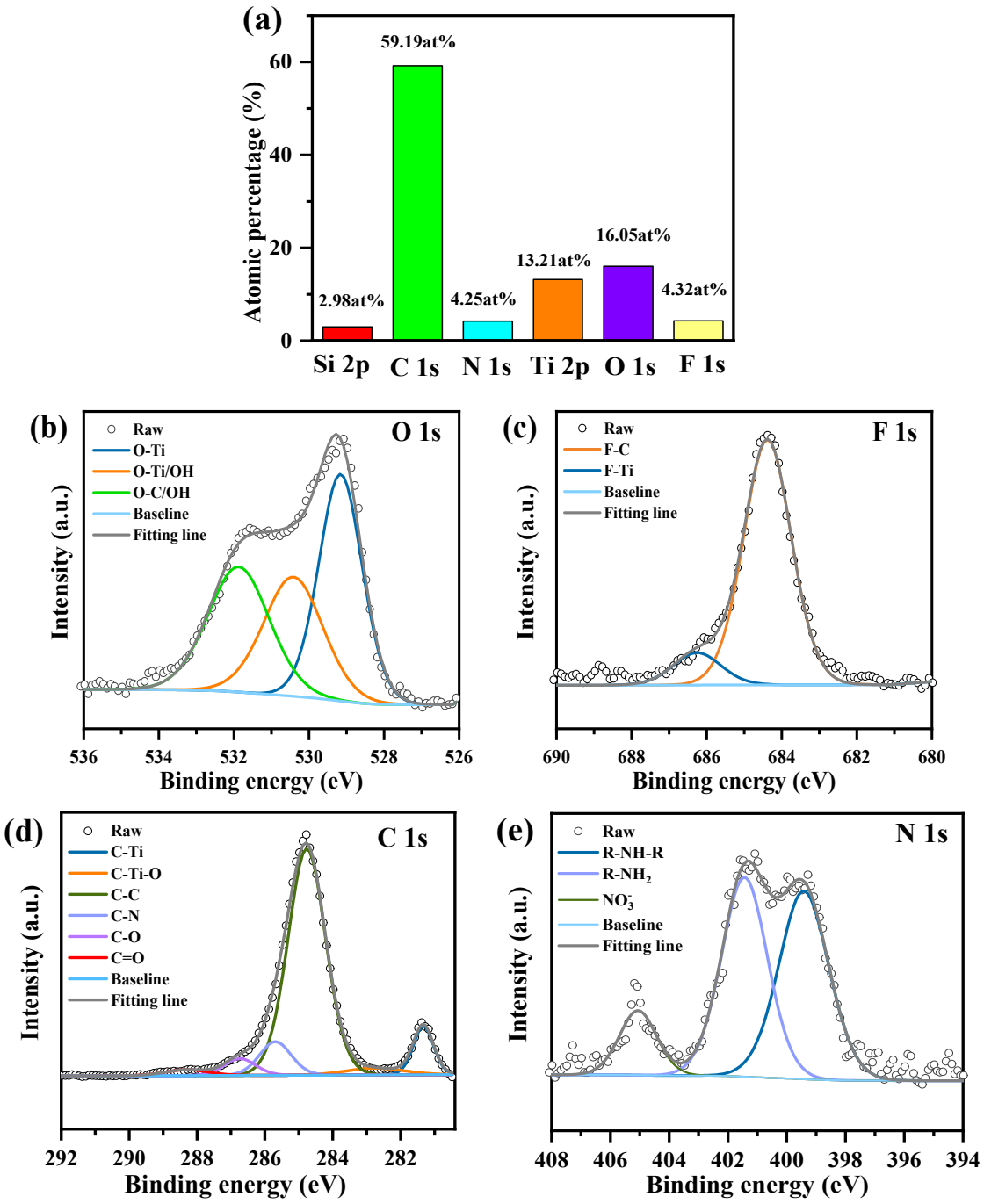

Fig. S2. (a) Atomic percentage of each element, and high-resolution XPS spectra of (b) O 2p, (c) F 1s, (d) C 1s, and (e) N 1s of TN-AEAPTMS.

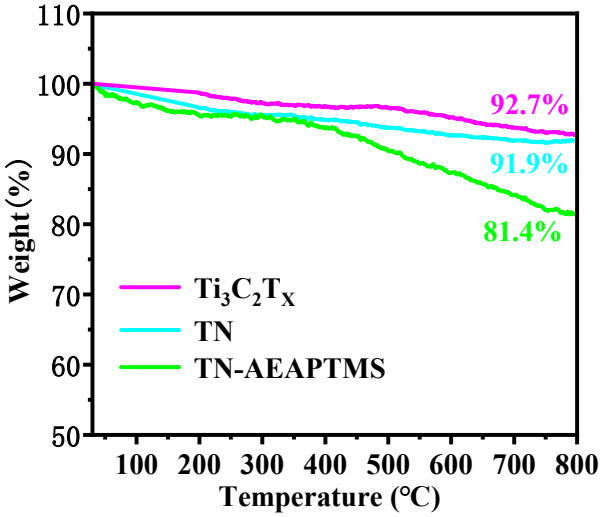

Fig. S3. TGA curves of Ti_3C_2Tx, TN and TN-AEAPTMS.

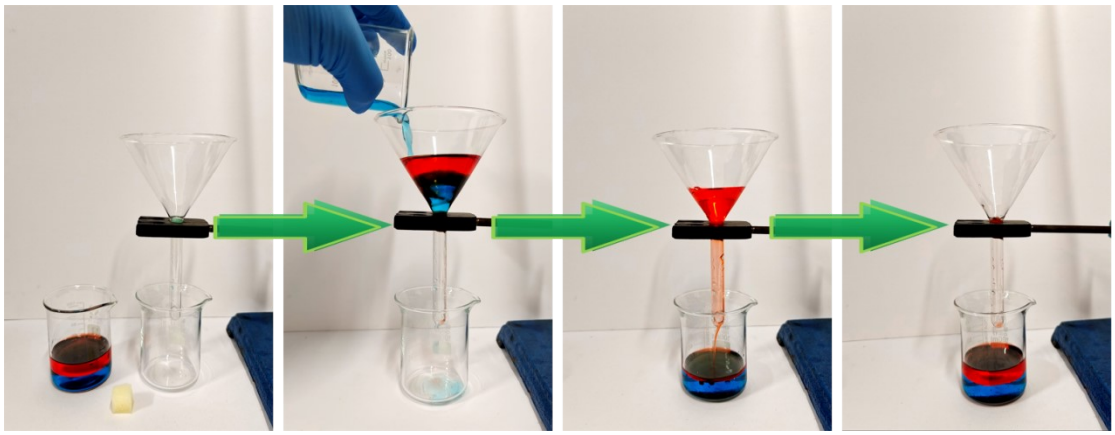

Fig. S4. Cyclohexane/water mixture separation process with the pristine PU.

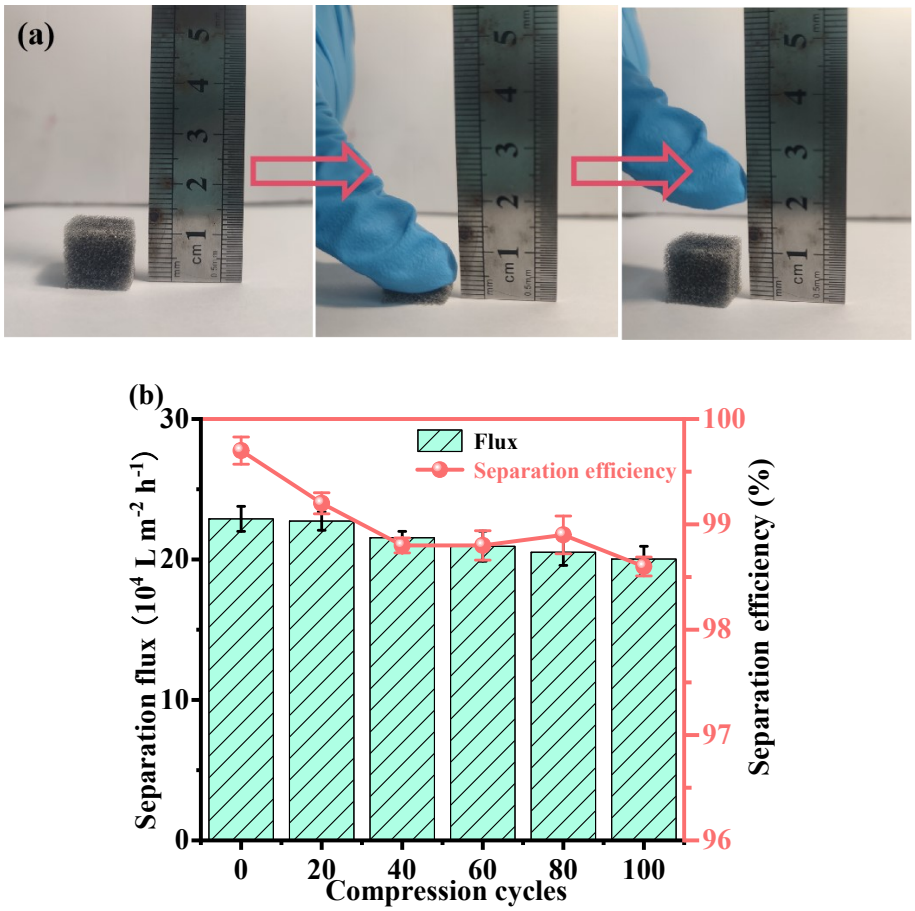

Fig. S5. (a) Photographs of TN-AEAPTMS@PU compression process, (b) Separation flux and separation efficiency of TN-AEAPTMS@PU at different compression times.

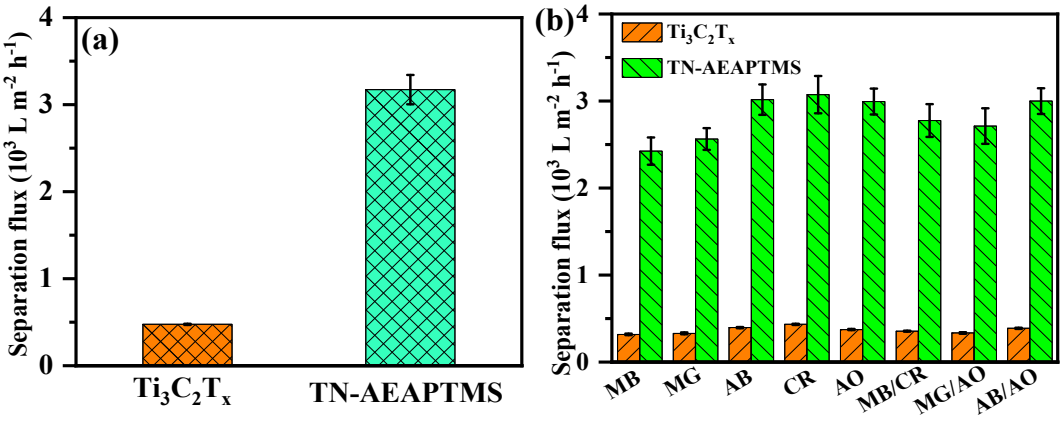

Fig. S6. (a) Pure water fluxes of $Ti_3C_2T_x$@MCE and TN-AEAPTMS@MCE, (b) Separation fluxes of various dye solutions for $Ti_3C_2T_x$@MCE and TN-AEAPTMS@MCE.

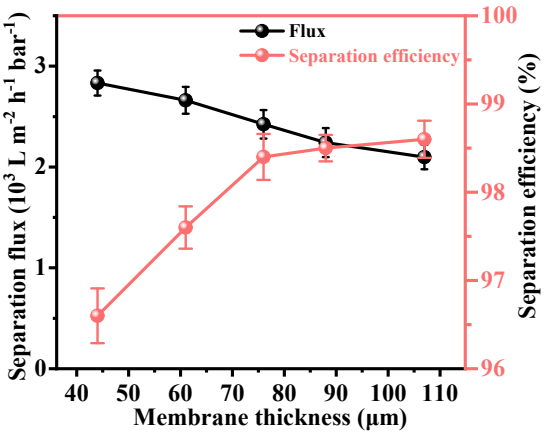

Fig. S7. Separation flux and separation efficiency of TN-AEAPTMS@MCE membrane with different membrane thickness.

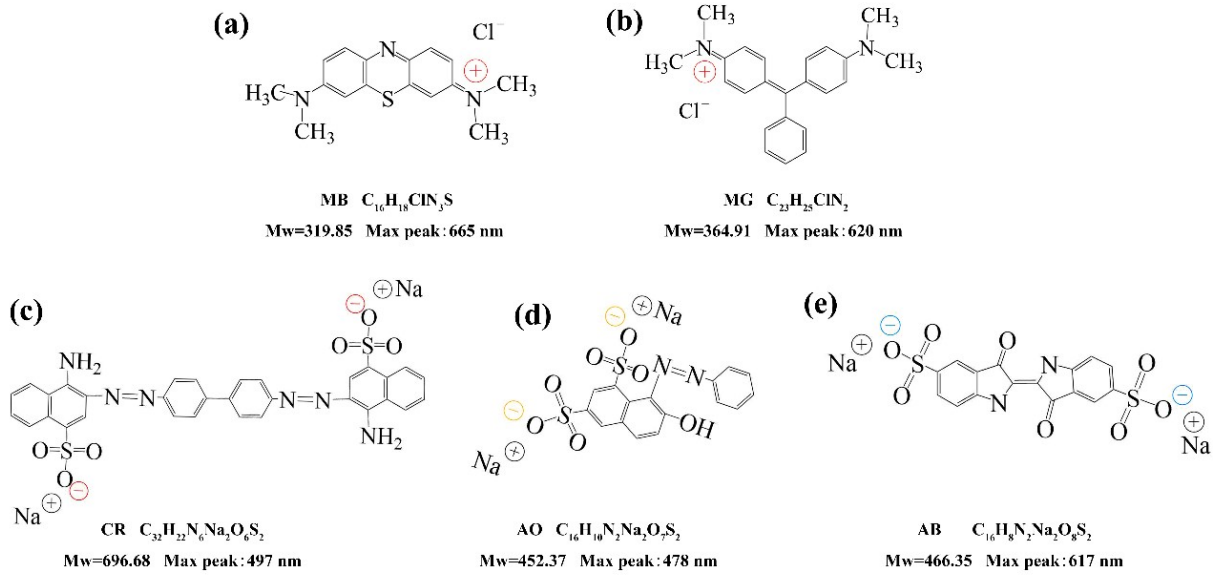

Fig. S8. Structure and molecular weight of different dye molecules.

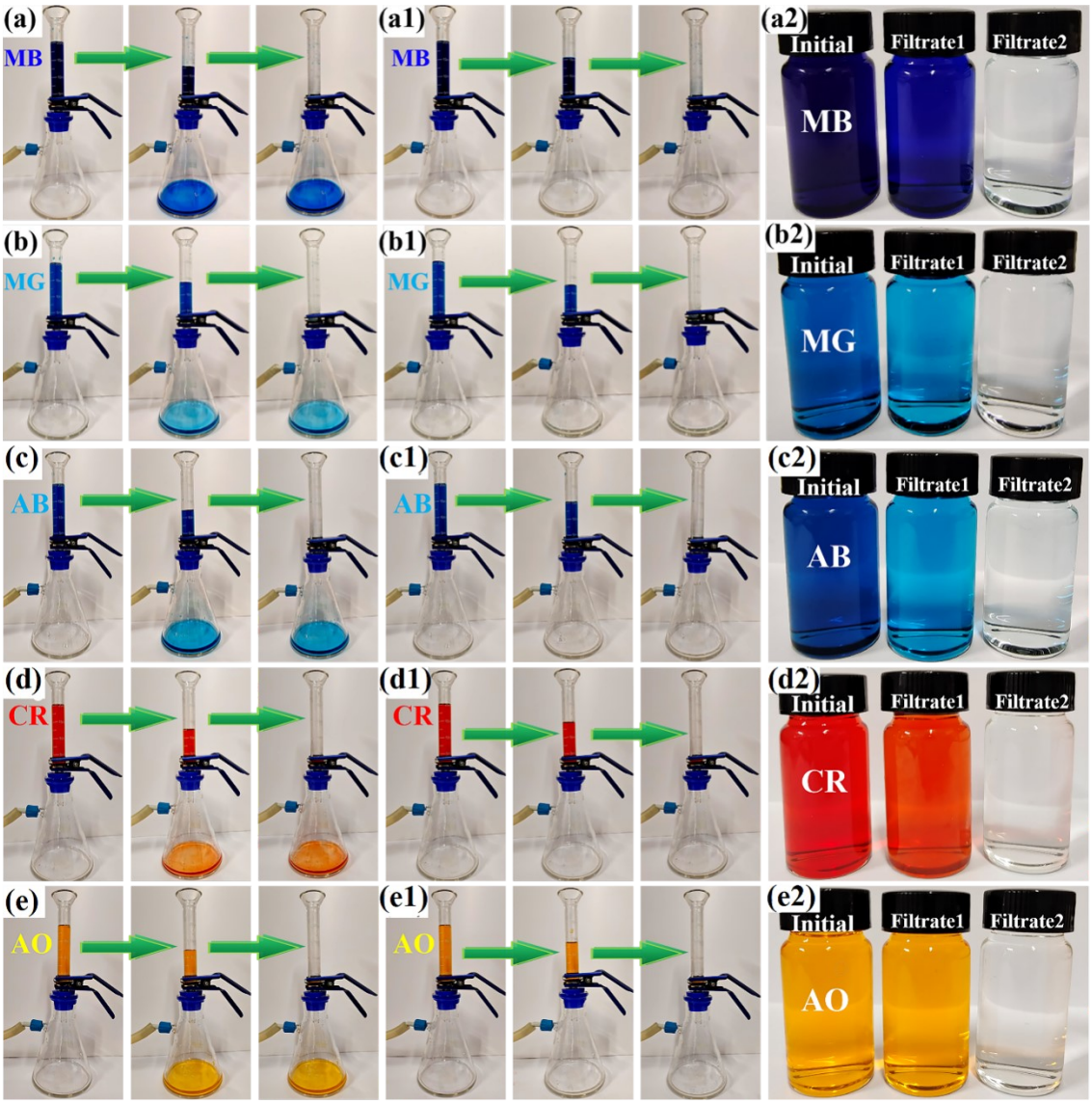

Fig. S9. Vacuum driven filtration of (a) MB, (b) MG, (c) AB, (d) CR and (e) AO aqueous solution on $Ti_3C_2T_x$@MCE, and (a1) MB, (b1) MG, (c1) AB, (d1) CR and (b1) AO aqueous solution on TN-AEAPTMS@MCE; (a2) MB, (b2) MG, (c2) AB, (d2) CR and (e2) AO aqueous solution, filtrate 1 (filtered through $Ti_3C_2T_x$@MCE) and filtrate 2 (filtered through TN-AEAPTMS@MCE).

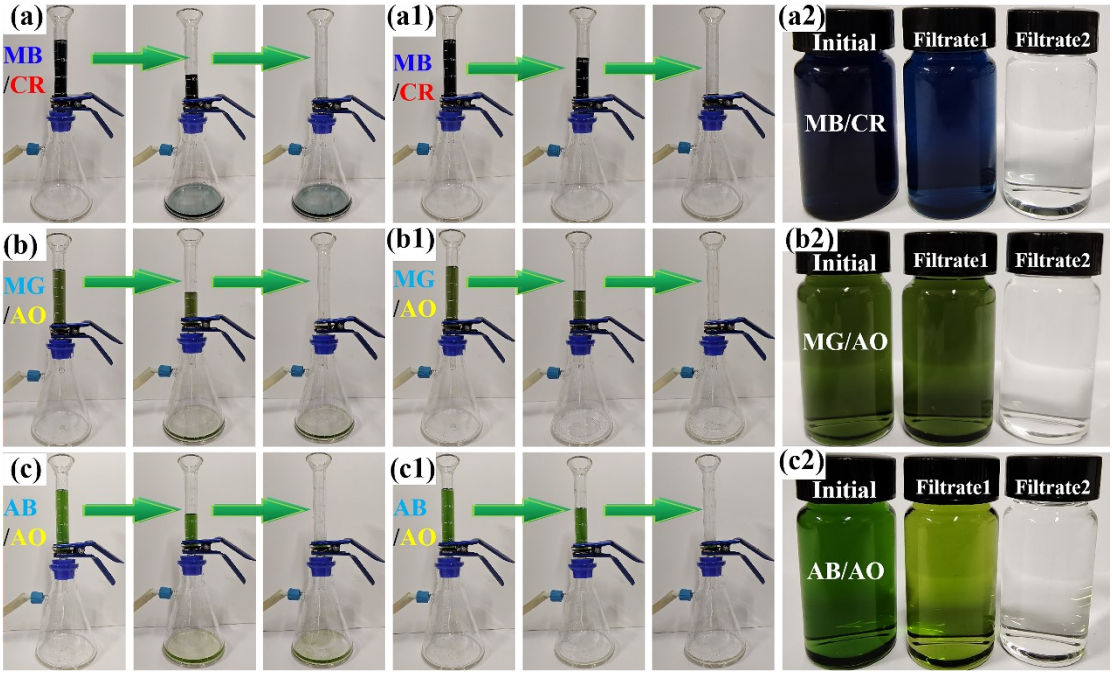

Fig. S10. Vacuum-driven filtration of (a) MB/CR, (b) MG/AO and (c) AB/AO mixed solutions on $Ti_3C_2T_x$@MCE, and (a1) MB/CR, (b1) MG/AO and (c1) AB/AO mixed solutions on TN-AEAPTMS@MCE; initial mixed solutions of (a2) MB/CR, (b2) MG/AO and (c2) AB/AO, filtrate 1 (filtered through $Ti_3C_2T_x$@MCE) and filtrate 2 (filtered through TN-AEAPTMS@MCE).

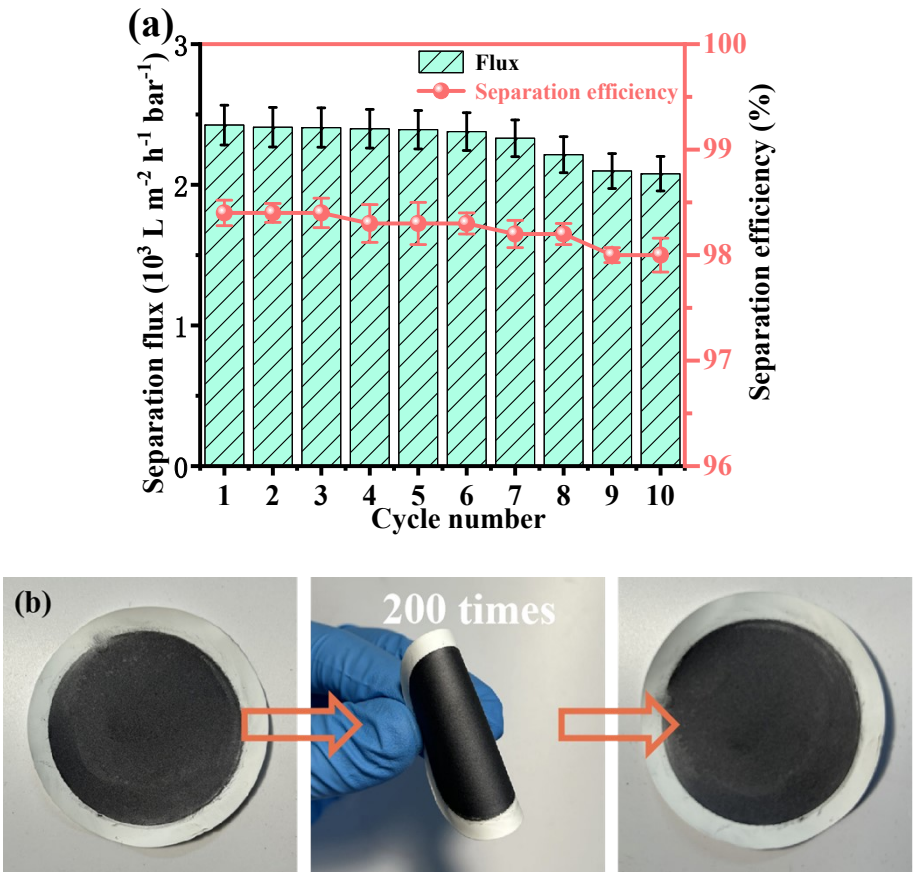

Figure S11. (a) Separation flux and separation efficiency of TN-AEAPTMS@MCE membrane after 10 cycles, (b) photographs of the TN-AEAPTMS@MCE membrane before and after bending over 200 cycles.

Table S1. γ^d and γ^p of water and ethylene glycol.

Wetting liquid	γ_l^d (mN m^{-1})	γ_l^p (mN m^{-1})
Water (W)	21.8	51.0
Ethylene glycol (E)	29.0	19.0

Table S2. Results of the calculated surface energies of the samples.

Sample	Water Contact Angle (°)	Glycol Contact Angle (°)	Dispersion component (mN m^{-1})	Polar component (mN m^{-1})	Suface energy (mN m^{-1})
PU	125.8	117.78	2.01	1.41	3.42
$Ti_3C_2T_x$@PU	89.31	83.01	2.52	16.02	18.54
TN@PU	37.14	34.77	2.22	67.01	69.23
TN-AEAPTMS@PU	0	0	1.98	86.02	87.99

Previous studies have shown that the wettability of materials is related to surface roughness and chemical composition.[1] Superhydrophilic/underwater superoleophobic materials usually have higher surface energy, which can be determined by the Owens-Wendt-Rabel-Kaelble (OWRK) method.[2]

$$(1+cos\theta)\gamma_1 = 2\sqrt{\gamma_s^d\gamma_1^d} + 2\sqrt{\gamma_s^p\gamma_1^p} \quad (1)$$

where θ is the contact angle of the liquid, γ^d and γ^p represent the surface energy of the dispersed part and the polar part. The subscripts s and l represent the solid and liquid phases, respectively.

According to the definition of the contact angle of underwater oil on the solid surface, the underwater oleophobic mechanism of TN-AEAPTMS@PU can be further explained.[3]

$$cos\theta_{o-w} = \frac{\gamma_{o-a}cos\theta_o - \gamma_{w-a}cos\theta_w}{\gamma_{o-w}} \quad (2)$$

where, $\gamma_{o\text{-}a}$, $\gamma_{w\text{-}a}$, and $\gamma_{o\text{-}w}$ represent the interfacial tensions of oil/air, water/air, and oil/water, respectively. $\theta_{o\text{-}a}$, $\theta_{w\text{-}a}$ and $\theta_{o\text{-}w}$ are the contact angles of oil in the air, water in air, and oil under water, respectively. It is worth mentioning that for the same oil, $\gamma_{o\text{-}a}$, $\gamma_{w\text{-}a}$, $\gamma_{o\text{-}w}$, and $\theta_{o\text{-}a}$ are constants. Therefore, $\theta_{o\text{-}w}$ increases as $\theta_{w\text{-}a}$ decreases.It is further demonstrated that the superhydrophilic TN-AEAPTMS@PU also possesses excellent underwater superoleophobicity.

Furthermore, the intrusion pressure can further explain the oil-water separation performance of the superwetted sponge.[4]

$$\Delta P = \frac{4\gamma_{lv}}{d} = \frac{C\gamma_{lv}cos\theta_{adv}}{A} \quad (3)$$

where $\theta_{adv,}$ $\gamma_{lv,}$ d, C, and A represent the advancing contact angle of liquid, the interfacial tension between liquid and vapor, the diameter, perimeter, and cross-sectional area of the meniscus, respectively.

References

[1] Y. Xu, G. Wang, L. Zhu, L. Shen, Z. Zhang, T. Ren, Z. Zeng, T. Chen, Q. Xue,J. Hazard. Mater., 2021, 407, 124374.

[2] S. Zarghami, T. Mohammadi, M. Sadrzadeh, B. Van Der Bruggen, Sci. Total Environ., 2020, 711, 134951.

[3] Z. Liao, G. Wu, D. Lee, S. Yang, ACS Appl. Mater. Interfaces., 2019, 11, 13642-13651.

[4] H. Cao, Y. Liu, J. Colloid Interface Sci., 2021, 598, 483-491.